molecular pharmaceutics

Article

pubs.acs.org/molecularpharmaceutics

Novel Bifunctional Cyclic Chelator for ^{89}Zr Labeling—Radiolabeling and Targeting Properties of RGD Conjugates

Chuangyan Zhai,[†,⊥] Dominik Summer,[†] Christine Rangger,[†] Gerben M. Franssen,[‡] Peter Laverman,[‡] Hubertus Haas,[§] Milos Petrik,[∥] Roland Haubner,[†] and Clemens Decristoforo*[,†]

[†]Department of Nuclear Medicine, Medical University Innsbruck, Innsbruck, Austria

[‡]Department of Radiology & Nuclear Medicine, Radboud University Medical Center, Nijmegen, The Netherlands

[§]Division of Molecular Biology, Medical University Innsbruck, Innsbruck, Austria

[∥]Institute of Molecular and Translational Medicine, Faculty of Medicine and Dentistry, Palacky University, Olomouc, Czech Republic

[⊥]Department of Nuclear Medicine, Guangdong General Hospital & Guangdong Academy of Medical Sciences, Guangzhou, China

Supporting Information

ABSTRACT: Within the last years ^{89}Zr has attracted considerable attention as long-lived radionuclide for positron emission tomography (PET) applications. So far desferrioxamine B (DFO) has been mainly used as bifunctional chelating system. Fusarinine C (FSC), having complexing properties comparable to DFO, was expected to be an alternative with potentially higher stability due to its cyclic structure. In this study, as proof of principle, various FSC-RGD conjugates targeting $\alpha_v\beta_3$ integrins were synthesized using different conjugation strategies and labeled with ^{89}Zr. *In vitro* stability, biodistribution, and microPET/CT imaging were evaluated using [^{89}Zr]FSC-RGD conjugates or [^{89}Zr]triacetylfusarinine C (TAFC). Quantitative ^{89}Zr labeling was achieved within 90 min at room temperature. The distribution coefficients of the different radioligands indicate hydrophilic character. Compared to [^{89}Zr]DFO, [^{89}Zr]FSC derivatives showed excellent *in vitro* stability and resistance against transchelation in phosphate buffered saline (PBS), ethylenediaminetetraacetic acid solution (EDTA), and human serum for up to 7 days. Cell binding studies and biodistribution as well as microPET/CT imaging experiments showed efficient receptor-specific targeting of [^{89}Zr]FSC-RGD conjugates. No bone uptake was observed analyzing PET images indicating high *in vivo* stability. These findings indicate that FSC is a highly promising chelator for the development of ^{89}Zr-based PET imaging agents.

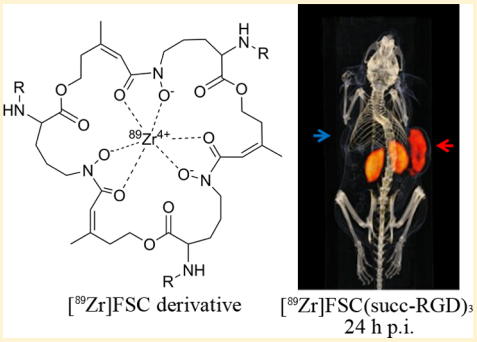

KEYWORDS: *fusarinine C, triacetylfusarinine C, ^{89}Zr, RGD peptide, positron emission tomography (PET)*

INTRODUCTION

Over the last years the positron-emitter ^{89}Zr has attracted considerable interest for molecular imaging applications using positron emission tomography (PET). In comparison to the commonly used radionuclides for PET (^{18}F, ^{68}Ga, ^{11}C, etc.), ^{89}Zr with its relatively long half-life of 78.4 h is particularly suited for *in vivo* imaging at late time-points. With a mean positron energy of 0.395 MeV, which is between the positron energies of ^{18}F (0.250 MeV) and ^{68}Ga (0.836 MeV), it allows for high resolution PET images for small animal imaging applications.[1]

For imaging applications at late time points ^{89}Zr has to be stably bound to a chelator to minimize dissociation *in vivo*, as free ^{89}Zr can accumulate in the bone or associate with plasma proteins. Over the years, several chelators, such as diethylenetriaminepentaacetic acid (DTPA), ethylenediaminetetraacetic acid (EDTA), and 1,4,7,10-tetraazacyclododecane *N*,*N*′,*N*″,*N*‴-tetraacetic acid (DOTA), have been evaluated with limited success.[2] Today desferrioxamine B (DFO) is the most prominent chelator for ^{89}Zr labeled biomolecules (Figure 1). [^{89}Zr]DFO mAb-conjugates have been used in a number of clinical trials for *in vivo* tracking and quantification of monoclonal antibodies (mAbs) by PET with good imaging quality. However, there are concerns about the stability of the complexes *in vivo* not only in relation to image quality but in particular to radiation dose. Several preclinical studies reported bone accumulation of dissociated ^{89}Zr ranging from 3 to 15% after 3 to 7 days.[3−8] Alternative chelators for ^{89}Zr^{4+} that could eliminate the release of osteophilic ^{89}Zr^{4+} and lead to safer PET procedures with reduced radiation dose and optimal image quality are required for the development of novel targeted PET-tracers.

Several studies have focused on the conjugation moiety[6,9,10] and recently also on the ligand itself.[11−15] Considering that DFO is a linear ligand and exposed to endogenous competitive cations and natural chelators *in vivo* that may challenge the

Received: February 11, 2015
Revised: April 8, 2015
Accepted: May 5, 2015
Published: May 5, 2015

DOI: 10.1021/acs.molpharmaceut.5b00128
Mol. Pharmaceutics 2015, 12, 2142−2150

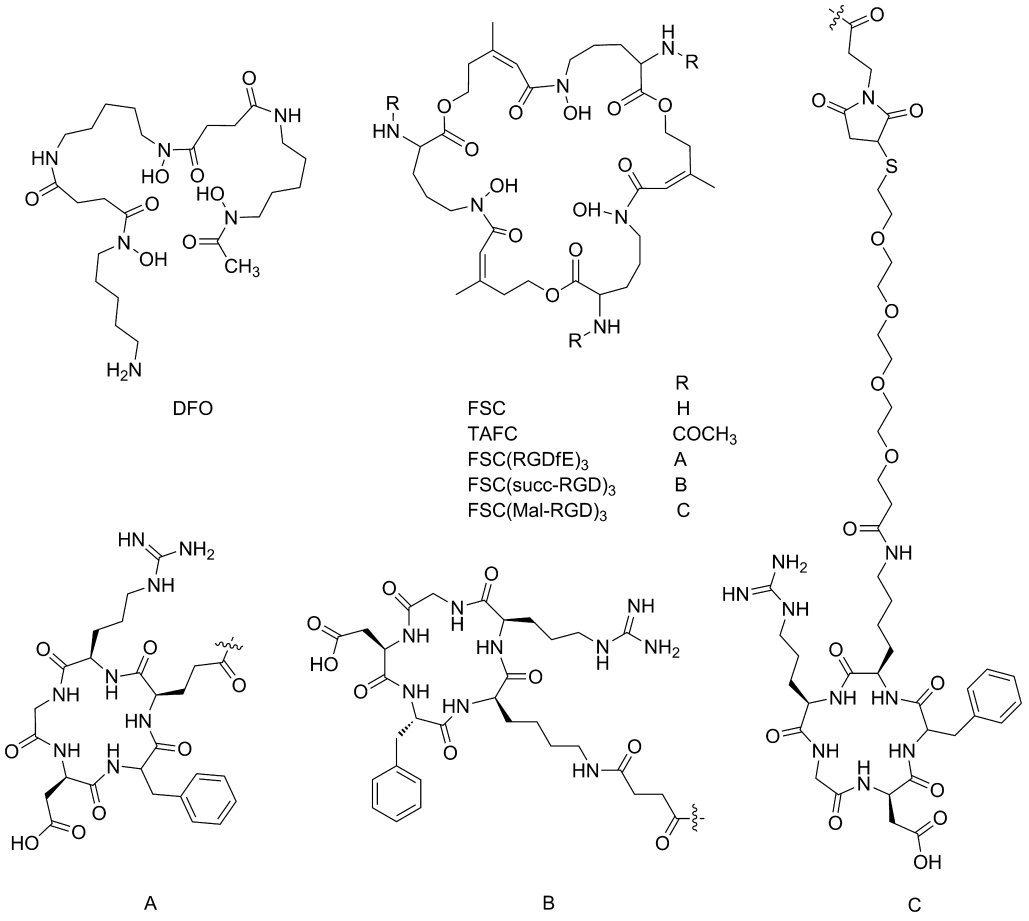

Figure 1. Chemical structures of DFO and FSC derivatives.

stability of the metal chelate, macrocyclic structures may favor a higher kinetic inertness of their metallic complexes.[16]

Recently we demonstrated that fusarinine C (FSC), a representative of the class of hydroxamate siderophores, is a promising bifunctional chelator for ^{68}Ga-radiolabeling (Figure 1).[17,18] FSC has three primary amines, which can be derivatized in a number of ways also applying the concept of multivalency. This is the combination of several targeting units in one single molecule. By attaching a cyclic RGD peptide, binding to $\alpha_v\beta_3$ integrins that are expressed during angiogenesis, via a succinic acid linker, stable [^{68}Ga]FSC(succ-RGD)$_3$ with excellent receptor binding properties and *in vivo* targeting was prepared. [^{68}Ga]FSC(succ-RGD)$_3$ showed superiority to monomeric cyclic RGD peptides, such as [^{18}F]Galacto-RGD and [^{68}Ga]-NODAGA-RGD. FSC has a similar structure like DFO with three hydroxamate groups providing six oxygen donors for metal binding. We postulated that FSC could be an alternative for ^{89}Zr labeling with complex formation properties comparable to DFO but potentially higher stability due to its cyclic structure. Thus, increased image contrasts at delayed time points are possible. In an initial study we could demonstrate that cyclic siderophores can be labeled with ^{89}Zr displaying comparable properties to its ^{68}Ga counterparts.[19]

In this study triacetylfusarinine C (TAFC), the triacetylated form of FSC, was investigated, and the labeling procedure and *in vitro* stability were compared with [^{89}Zr]DFO. Additionally, the feasibility of different FSC conjugation strategies, where the RGD peptides have been bound either directly or through a linker, has been evaluated. Moreover, radiolabeling properties, stability, and *in vivo* behavior of [^{89}Zr]FSC(succ-RGD)$_3$ in comparison to its ^{68}Ga labeled counterpart were compared. The study also included microPET/CT imaging in mice bearing $\alpha_v\beta_3$ integrin expressing tumor xenografts.

EXPERIMENTAL SECTION

General. All substances described were of reagent grade and were used without further purification. Human melanoma M21 and M21-L cells were a kind gift from D. A. Cheresh, Departments of Immunology and Vascular Biology, The Scripps Research Institute, La Jolla, CA, USA. ^{89}Zr was purchased from PerkinElmer, Inc. (USA). Analytical reversed-phase high performance liquid chromatography (RP-HPLC) analysis was performed using a Vydac 218 TP5215, 150 × 3.0 mm column (SRD, Vienna, Austria) at a flow rate of 1.0 mL/min with the following acetonitrile (CH_3CN)/H_2O/0.1% trifluoroacetic acid (TFA) gradients: 0−0.5 min 0% CH_3CN, 0.5−7.0 min 0−55% CH_3CN. Radiolabeling efficiency and radiochemical purity were determined by instant thin-layer chromatography (ITLC) on ITLC silica gel strips (Agilent Technologies) with 50 mM EDTA (pH 7, adjust pH using 10 M NaOH) as mobile phase. The strips were scanned using a mini-scan radio TLC scanner with flow-count detector (LabLogic, Sheffield, UK).

FSC and TAFC were prepared as described previously.[20] Briefly, the *Aspergillus* strains (*A. fumigatus* strain for FSC, *A. nidulans* strain for TAFC) were cultured in iron free minimal medium with 1% glucose for 36 h at 37 °C and 200 rpm. Biomass was removed by filtration, and the media-containing

DOI: 10.1021/acs.molpharmaceut.5b00128
Mol. Pharmaceutics 2015, 12, 2142−2150

siderophores were collected. TAFC was directly isolated by preparative RP-HPLC.

[Fe]Fusarinine C ([Fe]FSC). [Fe]FSC was prepared by saturating FSC solution with iron followed by purification using Amberlite XAD18 beads (Dow Chemical Company, Philadelphia, PA, USA) as column matrix. [Fe]FSC was further purified via preparative RP-HPLC and dried by lyophilization. Approximately 500 mg of a red colored solid was obtained. MALDI TOF-MS m/z $[M + H]^+$ = 780.4 [$C_{33}H_{51}FeN_6O_{12}$; exact mass, 779.3 (calculated)].

Peptide Synthesis. The cyclic pentapeptides cyclo(-Arg(Pbf)-Gly-Asp(OtBu)-DPhe-Lys-) (c(RGDfK) (Pbf, OtBu)) and cyclo(-Arg(Pbf)-Gly-Asp(OtBu)-DPhe-Glu-) (c-(RGDfE) (Pbf, OtBu)) (protecting groups: Pbf = 2,2,4,5,7-pentamethyl-3-hydrobenzofuran-6-sulfonyl; OtBu = *O-tert*-butyl) were prepared by cyclization of the side chain protected linear precursors, which were synthesized by Fmoc-based solid phase peptide synthesis (SPPS) as previously reported.[21] The Z-protecting group of lysine and ODmab of glutamic acid were cleaved by hydrogen with the Pd/C catalyst or 2% hydrazine in DMF, respectively. Pbf/OtBu was cleaved with a TFA/H_2O solution (v/v 95:5). A succinylated-derivative of c(RGDfK) (Pbf, OtBu) (succ-c(RGDfK) (Pbf, OtBu)) was synthesized using c(RGDfK) (Pbf, OtBu) reacting with molar excess of succinic anhydride.[17] The products were purified by preparative RP-HPLC, and their identities were confirmed by ESI-MS or MALDI TOF-MS. succ-c(RGDfK) (Pbf, OtBu), ESI-MS m/z $[M + H]^+$ = 1012.6 [$C_{48}H_{69}N_9O_{13}S$; exact mass, 1011.5 (calculated)]; c(RGDfE) (Pbf, OtBu), ESI-MS m/z $[M + H]^+$ = 913.4 [$C_{43}H_{60}N_8O_{12}S$; exact mass, 912.4 (calculated)]; c(RGDfK), MALDI TOF-MS $[M + H]^+$ = 604.9 [$C_{27}H_{41}N_9O_7$; exact mass, 603.3 (calculated)].

[Fe]FSC(RGDfE)$_3$ and [Fe]FSC(succ-RGD)$_3$. [Fe]FSC (10 mg, 12.8 μmol) and an excess of 5 equiv of succ-c(RGDfK) (Pbf, OtBu) (64.9 mg, 64.2 μmol) or c(RGDfE) (Pbf, OtBu) (58.5 mg, 64.2 μmol) were dissolved in 2 mL of DMF. After addition of 24.4 mg of HATU (64.2 μmol) and 8.7 mg of HOAt (64.2 μmol) and adjustment of the pH to 9 using DIPEA, the reaction mixture was stirred for 72 h at room temperature (RT). Hereafter, the volume of the solvent was reduced *in vacuo*, and the conjugate was precipitated using water. The crude [Fe]FSC(succ-RGD)$_3$ (Pbf, OtBu)) and [Fe]FSC(RGDfE)$_3$ (Pbf, OtBu) were dissolved in 2 mL of a solution composed of TFA/H_2O/triisopropylsilan in a ratio of 38:1:1. The reaction mixture was allowed to react for 1 h at RT. Subsequently, the solvent was reduced, and the crude product was obtained by precipitation using diethyl ether. Finally, the product was dried and purified via preparative RP-HPLC. [Fe]FSC(RGDfE)$_3$, yield 14.9 mg (5.9 μmol), 46%; MALDI TOF-MS $[M + H]^+$ = 2539.2 [$C_{111}H_{153}FeN_{30}O_{36}$; exact mass, 2538.0 (calculated)]; [Fe]FSC(succ-RGD)$_3$, yield 23.5 mg (8.3 μmol), 65%, MALDI TOF-MS $[M + H]^+$ = 2836.1 [$C_{126}H_{180}FeN_{33}O_{39}$; exact mass, 2835.2 (calculated)].

SAT(PEG)$_4$-RGD. c(RGDfK) (107 mg, 0.13 mmol) in 2 mL of DMF was mixed with 855 μL of *N*-succidimidyl-*S*-acetyl(thiotetraethylene glycol) (SAT(PEG)$_4$) stock solution in dimethyl sulfoxide (DMSO; 0.16 mmol, 1.2 equiv). The reaction mixture was alkalized to a pH of 9 using DIPEA and stirred for 2 h at RT. Subsequently, the solvent was reduced, and the conjugate was precipitated by addition of diethyl ether. Then, SAT-(PEG)$_4$-RGD was washed thrice with diethyl ether and was dried *in vacuo* to give the product as yellow oil with honey-like consistency. Yield 122 mg (0.13 mmol).

HS-(PEG)$_4$-RGD. SAT-(PEG)$_4$-RGD (12 mg, 55 μmol) was dissolved in 0.5 mL of phosphate buffered saline (PBS, pH 7.4), and 2 mL of 0.5 M hydroxylamine solution was added. The pH was adjusted to 6.0. After the mixture was stirred for 2 h at RT, HS-(PEG)$_4$-RGD was purified via preparative RP-HPLC and dried by lyophilization. Yield 42.9 mg (49.5 μmol), 90%, ESI-MS m/z $[M + H]^+$ = 868.5 [$C_{38}H_{61}N_9O_{12}S$; exact mass, 867.4 (calculated)].

Maleimide Derivatized [Fe]FSC ([Fe]FSC(Mal)$_3$). [Fe]FSC (10 mg, 12.8 μmol) and an excess of 5 equiv of 3-maleimidopropionic acid *N*-hydroxysuccinimide ester (17.1 mg, 64.2 μmol) was dissolved in 2 mL of DMF. The pH was adjusted to 8.0 using DIPEA, and the reaction mixture was stirred for 1.5 h at RT. Hereafter, [Fe]FSC(Mal)$_3$ was purified via preparative RP-HPLC. [Fe]FSC(Mal)$_3$, yield 12.7 mg (10.3 μmol), 80%, MALDI TOF-MS $[M + H]^+$ = 1234.1 [$C_{54}H_{66}FeN_9O_{21}$; exact mass, 1232.4 (calculated)].

[Fe]FSC(Mal-RGD)$_3$. HS-(PEG)4-c(RGD) (30 mg, 34.6 μmol) was dissolved in 1 mL PBS. [Fe]FSC(Mal)$_3$ (12.7 mg, 10.3 μmol) was dissolved in 200 μL of CH_3CN and added to the solution. After 30 min, the product was purified via preparative RP-HPLC and dried by lyophilization. Yield 30.5 mg (8.0 μmol), 78%.

Demetalation. [Fe]FSC(RGDfE)$_3$ (10 mg, 3.9 μmol), [Fe]FSC(succ-RGD)$_3$ (10 mg, 3.5 μmol) or [Fe]FSC(Mal-RGD)$_3$ (10 mg, 2.6 μmol) was dissolved in 40-fold of a disodium EDTA solution (25 mM, pH 4). After 1 h stirring at RT the solution was directly isolated via preparative RP-HPLC and dried by lyophilization. FSC(RGDfE)$_3$, yield 6.2 mg (2.5 μmol), 64%, MALDI-TOF-MS $[M + H]^+$ = 2487.8, [$C_{111}H_{156}N_{30}O_{36}$; exact mass, 2485.1 (calculated)]; FSC(succ-RGD)$_3$, yield 6.4 mg (2.3 μmol), 66%, MALDI-TOF-MS $[M + H]^+$ = 2785.0, [$C_{126}H_{183}N_{33}O_{39}$; exact mass, 2782.3-(calculated)]; FSC(Mal-RGD)$_3$, yield 6.8 mg (1.8 μmol), 69%, MALDI-TOF-MS $[M + H]^+$ = 3785.2 [$C_{168}H_{252}N_{36}O_{57}S_3$; exact mass, 3781.7 (calculated)].

^{89}Zr Radiolabeling. Approximately 30 MBq (30 μL) of ^{89}Zr-oxalate was transferred into a low-protein binding Eppendorf tube, followed by addition of 27 μL of 1 M sodium carbonate. The reaction solution was incubated for 3 min at RT. Thereafter, 100 μL of HEPES buffer (0.5 M, pH 7.0) was added to the reaction vial. DFO (32.8 μg), TAFC (42.6 μg), or the FSC-RGD conjugates [(FSC(RGDfE)$_3$, FSC(succ-RGD)$_3$, or FSC(Mal-RGD)$_3$); 30 μg] was added to the reaction vial. The pH of the reaction vial was measured to be sure that it was between 6.8 and 7.2. The solution was allowed to react at RT for 90 min. The reaction was monitored via ITLC (^{89}Zr-complexes remained at the origin and free ^{89}Zr migrates with the solvent front, see Supporting Information, Figure S1) and confirmed by HPLC. For animal experiments, after radiolabeling 60 μL of $CaCl_2$ (0.5 M) was added to the reaction vial, which resulted in a precipitate of Ca-oxalate. The solution was passed through a 0.2 μm filter to remove Ca-oxalate. The filtrate was diluted to an appropriate volume using saline for further evaluation.

Distribution Coefficient (logD). Aliquots of 50 μL of radioligand ([^{89}Zr]DFO, [^{89}Zr]TAFC, or [^{89}Zr]FSC-RGD conjugates) were diluted in 450 μL of PBS. Then 500 μL of octanol was added, and the mixture was vortexed for 15 min at 1400 rpm and centrifuged for 2 min at 2000 rcf. Subsequently, 50 μL aliquots of the aqueous and the octanol layer were collected, measured in the gamma counter, and logD values were calculated using Excel (n = 5).

DOI: 10.1021/acs.molpharmaceut.5b00128
Mol. Pharmaceutics 2015, 12, 2142−2150

Stability Assay. Determination of the stability of [^{89}Zr]-DFO, [^{89}Zr]TAFC, and [^{89}Zr]FSC-RGD conjugates was carried out by incubating the radioligands in PBS, 1000-fold molar excess of EDTA solution with different pH (pH 7 and pH 6; radioligand vs EDTA: 25 μM vs 25 mM) as well as in human serum for 7 days at 37 °C, respectively. At selected time points three aliquots of PBS and EDTA solution were analyzed directly via ITLC, while the three serum aliquots were mixed with 500 μL of CH_3CN, vortexed, and centrifuged at 20,000 rcf for 2 min prior to analysis.

Transchelation Study. [^{89}Zr]DFO and [^{89}Zr]TAFC (50 μL each) were mixed with a 1000-fold molar excess of either TAFC or DFO for 7 days at RT. At selected time points aliquots of the solutions were analyzed directly via RP-HPLC. ([^{89}Zr]DFO t_R = 4.8 min; [^{89}Zr]TAFC t_R = 5.9 min). The transchelation was determined by the ratio of [^{89}Zr]DFO and [^{89}Zr]TAFC. Three replicates were analyzed for each radioligand.

Protein Binding Assay. Protein binding abilities were evaluated by incubating [^{89}Zr]DFO and [^{89}Zr]TAFC for 7 days and [^{89}Zr]FSC-RGD conjugates for 4 h at 37 °C in fresh human serum. Subsequently, 30 μL of the solution was passed through a size exclusion spin column (MicroSpin G-50 column, GE healthcare, Buckinghamshire, UK) via centrifugation at 2000 rcf for 2 min. Protein binding of the conjugates in triplicates was determined by measuring the activity on the column (nonprotein bound) and the activity in the eluate (protein bound) in a gamma counter.

Internalization Assay. M21 cells ($\alpha_v\beta_3$ integrin positive) were diluted with RPMI 1640 (Gibco, Invitrogen Corporation, Paisley, UK) containing 1% glutamine (m/v), 1% bovine serum albumin (BSA) (m/v), $CaCl_2$ (1 mM), $MgCl_2$ (1 mM), and $MnCl_2$ (10 mM) to a concentration of 2.0 × 10^6 cells/mL. Aliquots of 1 mL cell solution were transferred to Eppendorf tubes for incubation at 37 °C for 1 h. After addition of [^{89}Zr]FSC(RGDfE)$_3$, [^{89}Zr]FSC(succ-RGD)$_3$, or [^{89}Zr]FSC-(Mal-RGD)$_3$ (approximately 1.5 × 10^6 cpm), the cells were incubated in triplicates with either PBS with 0.5% BSA (150 μL, total series) or with 10 μM c(RGDyV) in PBS/0.5% BSA (150 μL, nonspecific series) at 37 °C for 90 min. After the incubation time the tubes were centrifuged, and incubation was stopped by removal of the medium. Then the cells were washed twice with ice-cold TRIS-buffered saline. Subsequently, the cells were incubated two times in acid wash buffer (20 mM acetate buffer, pH 4.5) at 37 °C for 5 min. Then the tubes were centrifuged, and the supernatant was collected in plastic vials (membrane bound activity). In a last step the cells were lysed by addition of 2 M NaOH, and the radioactivity associated with cells was collected in plastic vials (internalized radioligand fraction). Protein content in the NaOH fraction was determined using a spectrometric method (Bradford assay). The internalized activity was calculated and expressed as percentage of total activity per milligram protein.

Biodistribution Studies. All animal experiments were conducted in compliance with the Austrian animal protection laws and with approval of the Austrian Ministry of Science (BMWF-66.011/000604-II/3*b*/2012 and BMWFW-66.011/0049-WF/II/3*b*/2014).

For the evaluation of biodistribution, four healthy female BALB/c mice (Charles River Laboratories, Sulzfeld, GER) were intravenously injected with [^{89}Zr]TAFC (~1.5 MBq/mouse, ~4 μg of precursor) into the tail vein and sacrificed at 6 h postinjection (p.i.). For the evaluation of tumor uptake of [^{89}Zr]FSC(succ-RGD)$_3$ female, athymic BALB/c nude mice (Charles River Laboratories) were used. For the induction of tumor xenografts mice were injected subcutaneously with 5 × 10^6 $\alpha_v\beta_3$ integrin positive M21 cells into the right hind limb and with 5 × 10^6 $\alpha_v\beta_3$ integrin negative M21-L cells (negative control) into the left hind limb of the same mouse (n = 4). The tumors were allowed to grow until they had reached a volume of 0.3 to 0.6 cm^3. On the day of the experiment [^{89}Zr]FSC-(succ-RGD)$_3$ (~0.5 MBq/mouse, ~0.5 μg of peptide) was intravenously injected in the lateral tail vein. Mice were sacrificed by cervical dislocation at 1, 2, and 4 h after injection. Organs (spleen, pancreas, stomach, intestine, kidney, liver, heart, and lung), blood, muscle tissue, bone, and tumors were dissected and weighted. As a comparison, four tumor-bearing mice were intravenously injected in the tail vein with [^{68}Ga]FSC(succ-RGD)$_3$ (~0.5 MBq/mouse, ~0.5 μg of precursor) and sacrificed at 1 h p.i. Activity of the different samples was measured in the gamma counter. Results were expressed as percentage of injected dose per gram tissue (% ID/g).

MicroPET/CT Imaging. MicroPET/CT imaging experiments were conducted on an Inveon microPET/CT scanner (Siemens Preclinical Solutions, Knoxville, USA). A group of four M21-tumor xenograft bearing BALB/c nude mice were administered with [^{89}Zr]FSC(succ-RGD)$_3$ (~5 MBq/mouse, ~5 μg of peptide) via intravenous tail vein injection. MicroPET images were acquired under general anesthesia (isoflurane/O_2) for 20 min. PET data for each mouse were recorded via static scans at 1, 4, and 24 h p.i. The microPET scans were reconstructed with Inveon Acquisition Workplace software (version 1.5; Siemens Preclinical Solutions), using a 3-dimensional fast maximum *a posteriori* algorithm with the following parameters: matrix, 256 × 256 × 161; pixel size, 0.4 × 0.4 × 0.8 mm; β-value of 1.5 mm resolution with uniform variance.

Statistical Analysis. Statistical analysis was performed using SPSS 17.0 software. The biodistribution data was analyzed using Student's t test. The level of significance was set at P = 0.05.

RESULTS

Precursor Synthesis. RGD peptides could be synthesized in good yields following standardized protocols.[21] Assemblies of the linear RGD peptides were accomplished on solid phase using Fmoc-protocols. Cyclization was carried out under high dilution conditions and subsequent Z-deprotection under hydrogen atmosphere for c(RGDfK)(Pbf, OtBu) or ODmab-deprotection with 2% hydrazine in DMF for c(RGDfE)(Pbf, OtBu). The lysine side chain was modified via addition of succinic anhydride enabling the coupling of the RGD peptide to the primary amino functions of [Fe]FSC. Amidation of succ-c(RGDfK)(Pbf, OtBu) or c(RGDfE)(Pbf, OtBu) with [Fe]FSC was accomplished via *in situ* activation using HATU/HOAt and DIPEA. Complete deprotection and subsequent demetalation of the organometallic complexes resulted in an average yield of approximately 40% and 30% for FSC(succ-RGD)$_3$ and FSC(RGDfE)$_3$, respectively. [Fe]-FSC(Mal)$_3$ was synthesized by [Fe]FSC reaction with 3-maleimidopropionic acid *N*-hydroxysuccinimide ester. The deprotected c(RGDfK) was modified with SAT(PEG)$_4$ and then treated with hydroxylamine for 20 min to expose the sulfhydryl group for coupling [Fe]FSC(Mal)$_3$ at neutral pH, resulting in an average yield of 55%. The removal of [Fe],

DOI: 10.1021/acs.molpharmaceut.5b00128
Mol. Pharmaceutics 2015, 12, 2142−2150

which was used to protect the complexing moiety, from [Fe]FSC-RGD conjugates was carried out using 40-fold molar excess of EDTA solution at pH 4 within 25 to 60 min with high yield (>90%). The rapid disappearance of the intense red color of the solution indicated the successful removal of [Fe]. After HPLC purification the chemical purity of the final compounds was >95%.

^{89}Zr Radiolabeling. Labeling of DFO, TAFC, and the FSC-RGD conjugates with ^{89}Zr-oxalate was performed with slight modifications as described recently.[22] Radiolabeling was carried out in HEPES buffer at RT at pH 6.8 to 7.2. FSC could acquire ^{89}Zr quantitatively from ^{89}Zr-oxalate at RT with incubation times between 30 and 90 min depending on the concentration of precursor. Moreover, 1 μg of TAFC could be quantitatively labeled with 30 MBq of ^{89}Zr-oxalate leading to a specific activity of 25 GBq/μmol (without optimization). The time course of ^{89}Zr-complexation of FSC(succ-RGD)$_3$ (30 μg, 58 μM) is shown in Figure 2. Oxalate, which could be toxic due to the production of solid calcium oxalate causing kidney failure, was readily removed by preprecipitation with $CaCl_2$ and filtration using a 0.2 μm filter for *in vivo* experiments.

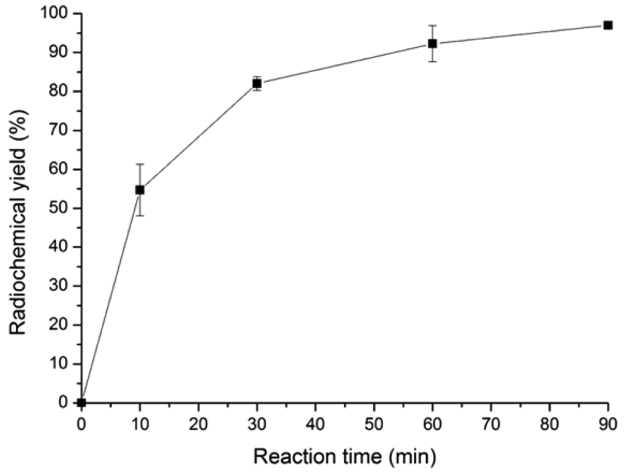

Figure 2. Time course of ^{89}Zr complexation of FSC(succ-RGD)$_3$ (58 μM, pH 7, at RT).

***In Vitro* Characterization.** [^{89}Zr]DFO, [^{89}Zr]TAFC, and [^{89}Zr]FSC-RGD conjugates showed high stability in PBS and human serum over a period of 7 days, and no demetalation was observed. LogD and protein binding data are summarized in Table 1. High hydrophilic character was observed for [^{89}Zr]FSC-RGD conjugates (logD was between −2.9 and −3.0). The lower hydrophilicity of [^{89}Zr]TAFC (logD −2.0) is in accordance with the data found for [^{68}Ga]TAFC.[23] The low protein-bound activity (<10%) over the whole monitoring period further confirmed the stability of FSC in human serum.

Table 1. LogD and Binding Properties of [^{89}Zr]DFO, [^{89}Zr]TAFC, and [^{89}Zr]FSC-RGD Conjugates

^{89}Zr complex	logD (pH 7.4)	incubation time (h)	protein binding (%)
[^{89}Zr]DFO	−3.0 ± 0.1	168	8.7 ± 1.0
[^{89}Zr]TAFC	−2.0 ± 0.0	168	6.8 ± 0.5
[^{89}Zr]FSC(RGDfE)$_3$	−3.0 ± 0.0	4	5.0 ± 0.8
[^{89}Zr]FSC(succ-RGD)$_3$	−2.9 ± 0.1	4	7.3 ± 0.5
[^{89}Zr]FSC(Mal-RGD)$_3$	−2.9 ± 0.2	4	6.0 ± 1.5

Stability data of [^{89}Zr]DFO, [^{89}Zr]TAFC, and [^{89}Zr]FSC(succ-RGD)$_3$ in 1000-fold molar excess of EDTA solution with different pH and transchelation data are summarized in Table 2. Based on ITLC analysis TAFC showed no transchelation in EDTA solution at pH 7 and minor transchelation (5.2%) at pH 6 after 7 days. [^{89}Zr]FSC(succ-RGD)$_3$ exhibited 4.4% transchelation, indicating high *in vitro* stability of the ^{89}Zr-FSC complex. In contrast, [^{89}Zr]DFO showed nearly 60% transchelation in EDTA at pH 7 after 7 days and more than 90% transchelation at pH 6 after 3 days. The superior stability of [^{89}Zr]FSC was also confirmed by the transchelation study, in which 100% of [^{89}Zr]DFO transchelated in 1000-fold molar excess of TAFC within 1 h, whereas 40% of [^{89}Zr]TAFC remained intact in 1000-fold molar excess of DFO after 7 days.

By incubating [^{89}Zr]FSC-RGD conjugates with $\alpha_v\beta_3$ integrin positive M21 cells and carrying out corresponding blocking studies [22 μmol of c(RGDyV)] the internalization ability of the multimeric RGD peptides was determined (Figure 3). The internalized activities were 2.3 ± 0.3% for [^{89}Zr]FSC(RGDfE)$_3$, 2.1 ± 0.3% for [^{89}Zr]FSC(succ-RGD)$_3$, and 1.6 ± 0.1% for [^{89}Zr]FSC(Mal-RGD)$_3$ of total activity per milligram protein (% cpm/mg). The corresponding activities were reduced to 0.2 to 0.3% cpm/mg of the reference activity via addition of excess of c(RGDyV), which demonstrated receptor-specific binding.

Biodistribution Studies. [^{89}Zr]TAFC showed rapid pharmacokinetics in normal mice at 6 h p.i. with fast blood clearance (0.05 ± 0.01% ID/g), low uptake of bone (0.04 ± 0.02% ID/g), and predominant renal excretion with some retention at this late time point (0.86 ± 0.48% ID/g). Biodistribution and specific tumor uptake of [^{89}Zr]FSC(succ-RGD)$_3$ were investigated at 1, 2, and 4 h postinjection in BALB/c nude mice bearing M21 ($\alpha_v\beta_3$ integrin positive) as well as M21-L ($\alpha_v\beta_3$ integrin negative) tumor xenografts (n = 4) (Figure 4). The uptake of [^{89}Zr]FSC(succ-RGD)$_3$ in the $\alpha_v\beta_3$ integrin positive M21 tumor was 2.83 ± 0.60% ID/g at 1 h p.i. At 2 h a slight increase to the maximum uptake of 3.48 ± 0.45% ID/g was seen and a slow clearance to 2.86 ± 0.30% ID/g at 4 h p.i. In contrast, a constant but low uptake (0.5% ID/g) was observed at all time points in the contralateral $\alpha_v\beta_3$ integrin negative M21-L tumors. This highly significant difference in tumor uptake between receptor-positive and receptor-negative tumors confirmed the receptor-selective uptake found *in vitro*. The fast blood clearance (0.16 ± 0.04% ID/g, 0.15 ± 0.0% ID/g, and 0.10 ± 0.01% ID/g at 1, 2, and 4 h p.i., respectively) led to an increased tumor/blood ratio. The comparably high activities in kidneys (6.42 ± 0.72% ID/g, 5.77 ± 0.20% ID/g, and 5.26 ± 0.90% ID/g at 1, 2 and 4 h p. i., respectively) could be related to renal excretion and partial retention. Notably, the low amount of activity in the bone remained stable (0.71 ± 0.05% ID/g, 0.79 ± 0.28% ID/g, and 0.73 ± 0.27% ID/g at 1, 2, and 4 h p. i., respectively) indicating the high *in vivo* stability of [^{89}Zr]FSC(succ-RGD)$_3$. Compared with the biodistribution data of [^{68}Ga]FSC(succ-RGD)$_3$ at 1 h, significant differences of uptake in blood, spleen, liver, and M21-L tumors were observed. The higher uptakes of [^{68}Ga]FSC(succ-RGD)$_3$ in the spleen (3.27 ± 0.64% ID/g vs 1.78 ± 0.22% ID/g) and in M21-L tumors (1.10 ± 0.30% ID/g vs 0.50 ± 0.12% ID/g) are related to the prolonged presence of the ^{68}Ga-tracer in the blood (0.63 ± 0.26% ID/g vs 0.16 ± 0.04% ID/g).

A microPET/CT imaging study with tumor-bearing nude mice was performed in order to investigate the *in vivo* pharmacokinetics of [^{89}Zr]FSC(succ-RGD)$_3$ (Figure 5). Again images confirmed receptor-specific activity accumulation

DOI: 10.1021/acs.molpharmaceut.5b00128
Mol. Pharmaceutics 2015, 12, 2142−2150

Table 2. Stability and Transchelation Studies of [^{89}Zr]DFO, [^{89}Zr]TAFC, and [^{89}Zr]FSC-RGD Conjugates (n = 3)

			% intact starting species by incubation time					
starting complex	competitor (1000-fold excess)	pH	1 h	4 h	1 d	3 d	5 d	7 d
[^{89}Zr]DFO	EDTA	7	95.5 ± 0.5	76.0 ± 1.0	55.4 ± 3.2	41.0 ± 5.2	43.3 ± 2.5	42.2 ± 2.3
		6	94.6 ± 0.4	63.5 ± 3.6	38.2 ± 8.4	6.4 ± 2.0	6.0 ± 1.8	
	TAFC	6	0.0 ± 0.0					
[^{89}Zr]TAFC	EDTA	7	99.6 ± 0.1	99.6 ± 0.1	99.3 ± 0.2	96.9 ± 0.3	98.3 ± 0.1	97.2 ± 0.2
		6	99.0 ± 0.1	98.1 ± 0.2	96.0 ± 0.6	94.7 ± 0.3	95.9 ± 0.3	94.4 ± 0.5
	DFO	6	96.7 ± 0.2	91.9 ± 0.3	74.2 ± 3.0	53.0 ± 4.1	43.3 ± 3.5	39.8 ± 2.0
[^{89}Zr]FSC(succ-RGD)$_3$	EDTA	7	98.2 ± 0.1	98.2 ± 0.1	96.5 ± 0.5	96.0 ± 0.4	94.5 ± 0.3	93.9 ± 0.7

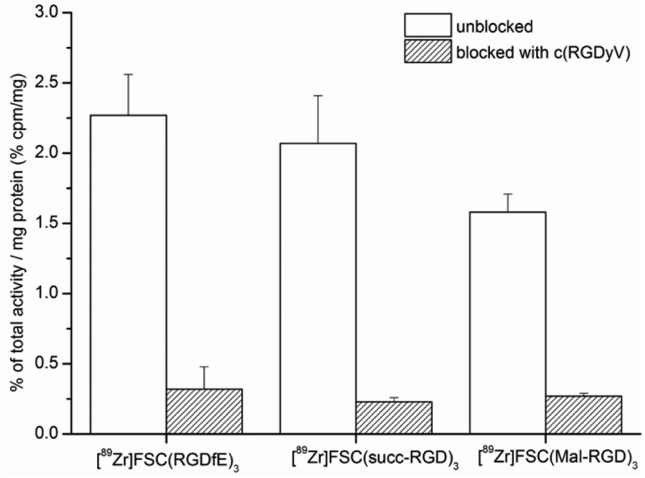

Figure 3. Internalization of [^{89}Zr]FSC(RGDfE)$_3$, [^{89}Zr]FSC(succ-RGD)$_3$, and [^{89}Zr]FSC(Mal-RGD)$_3$ in $\alpha_v\beta_3$ integrin positive M21 tumor cells.

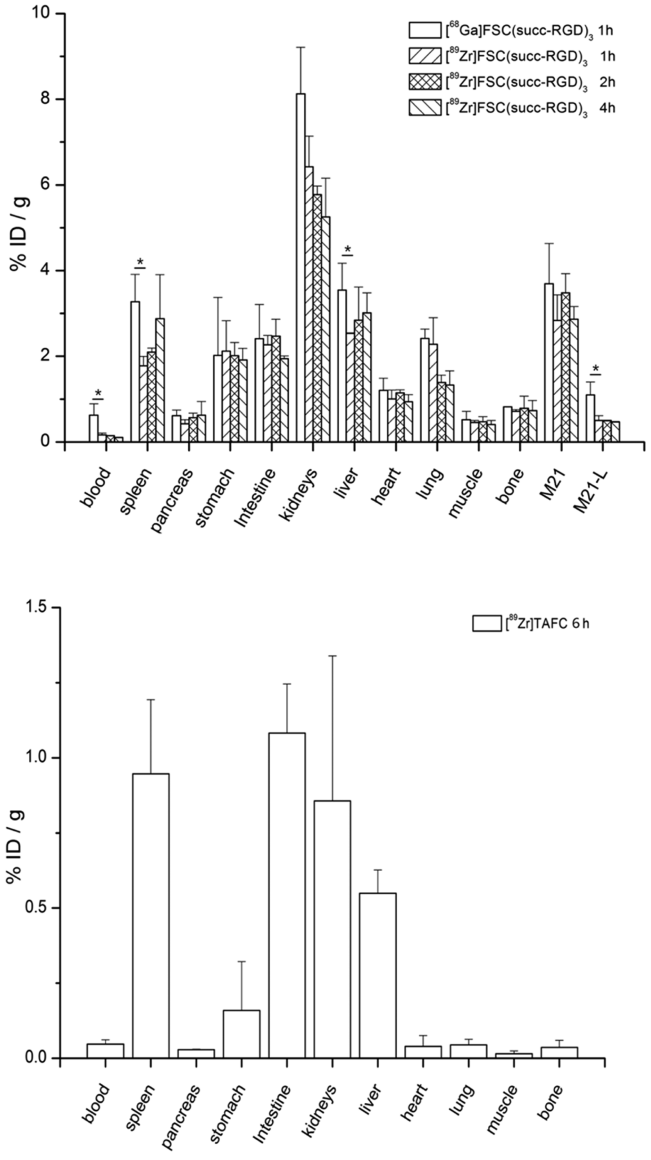

Figure 4. Biodistribution of [^{89}Zr]/[^{68}Ga]FSC(succ-RGD)$_3$ at 1, 2, and 4 h p.i. in BALB/C nude mice bearing the $\alpha_v\beta_3$ integrin positive M21 cell tumor on the right flank and the $\alpha_v\beta_3$ integrin negative control tumor M21-L on the left flank, and [^{89}Zr]TAFC at 6 h in normal BALB/c mice. Significant differences in uptake are marked with an asterisk (P = 0.05). Each data point represents an average of biodistribution data in four animals (n = 4).

in the $\alpha_v\beta_3$ integrin positive M21 tumors, and more importantly, no bone uptake was observed, confirming high *in vivo* stability of the compound. The M21 tumors could be clearly visualized over the whole monitoring period of 24 h, whereas the $\alpha_v\beta_3$ integrin negative M21-L tumors showed no uptake confirming the high specificity of [^{89}Zr]FSC(succ-RGD)$_3$. Besides the M21 tumors, only kidneys were visible, which is related to excretion and kidney retention.

DISCUSSION

The positron-emitting radionuclide ^{89}Zr is increasingly used for molecular imaging with PET; its clinical application is currently limited to conjugates using DFO as chelator. Even though several antibodies conjugated to DFO and radiolabeled with ^{89}Zr achieved some successful results, dissociation of ^{89}Zr *in vivo* has been observed indicating limited *in vivo* stability. Therefore, increasing efforts are made to design and synthesize novel robust and stable chelators for ^{89}Zr. The design of an ideal chelator is affected by many factors, such as the type and number of coordinated atoms, acyclic vs cyclic constructs, ring size, etc. Even the charge of the metal-complex may influence the biodistribution of a corresponding tracer labeled with a radiometal.

Based on the knowledge on structure, synthesis, and labeling of DFO-conjugates, the natural siderophore FSC was chosen as the starting point for our research. FSC is produced by fungi for acquiring iron from the environment and has been proven to be an excellent bifunctional chelator for ^{68}Ga in our laboratory.[17] Therefore, FSC, having three hydroxamic acid moieties similar to those of DFO, embedded in a cyclic structure, was expected to be an interesting alternative for ^{89}Zr labeling. In our study, TAFC was initially chosen to explore the labeling procedure and to evaluate the *in vitro* stability. It was labeled with ^{89}Zr-

DOI: 10.1021/acs.molpharmaceut.5b00128
Mol. Pharmaceutics 2015, 12, 2142−2150

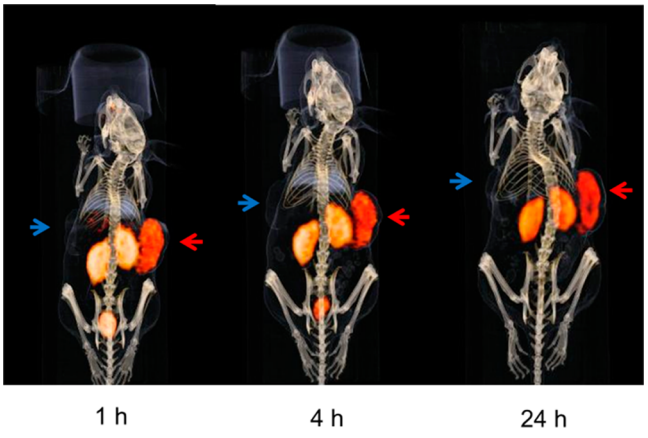

Figure 5. Three-dimensional volume projections of fused microPET/CT images of M21/M21-L tumor xenograft bearing nude mouse ([^{89}Zr]FSC(succ-RGD)$_3$, 5 μg, 5 MBq) at 1, 4, and 24 h p.i. Red arrow, $\alpha_v\beta_3$ integrin positive M21 tumor; blue arrow, $\alpha_v\beta_3$ integrin negative M21-L tumor.

oxalate following the established protocol found for [^{89}Zr]-DFO.[22] The cyclic structure of TAFC exhibits excellent complexation ability with quantitative complexation of ^{89}Zr from ^{89}Zr-oxalate between 30 to 90 min. This resulted in highly hydrophilic [^{89}Zr]TAFC and [^{89}Zr]FSC-RGD conjugates with low partition coefficients, indicating advantageous properties of these compounds for PET imaging. However, initial experiments using macroscale amounts of $ZrCl_4$ demonstrate that TAFC can, in contrast to DFO and other chelators that use ^{89}Zr-oxalate at pH 6.8−7.2 and reaction times between 1 to 2 h,[11] quantitatively form complexes at acidic pH (1−5) within 5 min (data not shown). This indicates that the chloride form of ^{89}Zr could be the better choice for labeling reactions. Moreover, it would avoid the use of highly concentrated solutions of oxalate, which is potentially toxic.

One of the main attractions of FSC-based constructs for ^{89}Zr radiolabeling lies in its excellent stability in challenging solution. [^{89}Zr]TAFC remained stable toward challenge with 1000-fold molar excess of EDTA and only limited transchelation was found after days of incubation with 1000-fold molar excess of DFO. In comparison [^{89}Zr]DFO revealed rapid transchelation toward EDTA even at pH 7 and complete transmetalation toward TAFC (both 1000-fold molar excess) within hours. This high stability of the [^{89}Zr]FSC structure was further confirmed by the studies with the [^{89}Zr]FSC-RGD conjugates. Additionally, as the pH in tumors (approximately pH 6.5) is lower than in healthy tissue, the observed high stability of [^{89}Zr]TAFC in slightly acidic conditions (pH 6) may be beneficial in particular for cancer imaging.

Inspired by the promising results found for [^{89}Zr]TAFC, the potential use of FSC conjugated to targeting vectors was investigated. For several reasons cyclic RGD pentapeptides were chosen as model vectors. First, RGD-peptides are very stable *in vitro* and *in vivo* and, more important, tolerate a variety of modifications at position 5 in the amino acid sequence without losing binding affinity.[24] Second, rapid predominantly renal excretion with low background activity is described for a big variety of different tracer based on this pentapeptide allowing an easier monitoring of the distribution of fragments based on rapid degradation in the body and especially in the bone.[25] Third, it is a well-known class of tracer where a great set of data is available.[26,27] Fourth, it is known that binding affinity and imaging properties of this tracer class benefit from the so-called multimerization approach.[28] Due to the fact that FSC includes three primary amine functions, this chelator allows conjugation of up to three ligands making them, besides working as chelator for the radiometal, an ideal scaffold for such approaches. Thus, this option additionally increases potential applications of FSC and derivatives. Anyway, it has to be pointed out that only small peptides may benefit from such a multimerization approach and not antibodies, which is the main field of application of ^{89}Zr-labeling. Nevertheless, it has been demonstrated by using, e.g., ^{64}Cu-NODAGA-RGD that tumor-to-background ratios further improve with prolonged imaging time making labeling of this peptide class with ^{89}Zr not *per se* uninteresting.[29]

As a proof of concept, different cyclic RGD pentapeptides were synthesized, and versatile conjugation strategies were explored. FSC(succ-RGD)$_3$ was synthesized using a succinic acid linker by amidation with a yield of 40%. In another approach c(RGDfÉ) was directly conjugated via the glutamic acid carboxylate to the chelator. This approach reduces the synthesis steps but also resulted in a lower yield possibly related to steric effects. In a third approach the maleimide−thiol strategy was introduced. This is a well-established technique and allows fast and mild reaction conditions in aqueous solution, facilitating the site specific conjugation of peptides and antibodies, which might be not stable under harsh conditions. Thus, the PEG-modified RGD-peptide could be coupled with even higher yield as found for the other two derivatives under mild conditions with the FSC derivative.

Biological properties of [^{89}Zr]FSC(succ-RGD)$_3$ were comparable to the properties of [^{68}Ga]FSC(succ-RGD)$_3$, which has clearly shown the advantage of multivalency through remarkable improvement of internalized activity *in vitro* and tumor uptake *in vivo* in our previous study.[17] An exception was the lower activity concentration in blood resulting in better tumor/blood ratios for the ^{89}Zr compound in comparison with the ^{68}Ga-labeled analogue, indicating an excellent *in vivo* stability of [^{89}Zr]FSC(succ-RGD)$_3$. The high stability was confirmed by microPET/CT imaging using the same murine tumor model. These studies clearly demonstrated no uptake in bone and high uptake in α_vß$_3$ integrin positive M21 tumors. A reason for the superior properties of [^{89}Zr]FSC(succ-RGD)$_3$ compared with [^{68}Ga]FSC(succ-RGD)$_3$ could partially be to the difference in the charge, having been reported to potentially influence excretion patterns of such biomolecules.[30]

The preferred coordination number for ^{89}Zr is eight, which was confirmed recently.[31] Certain developments aim on the design and synthesis of novel both octadentate and oxygen-rich Zr^{4+} chelates to achieve superior stabilities to DFO. Both Deri et al. and Patra et al. reported two kinds of linear octadentate chelators named HOPO and DFO*.[11,12] Guérard et al. also described a cyclic octadentate tetrahydroxamic acid chelator (*C7*).[13] *In vitro* studies of all three octadentate ligands showed improved stability. However, HOPO and *C7* lack the pendant group for coupling it to a targeting molecule. DFO* was linked to the bombesin peptide analogue [Nle^{14}]BBS(7−14), but was only investigated *in vitro*. [^{89}Zr]TAFC and *C7*, both have a 36-membered ring but different coordination numbers for ^{89}Zr. Nevertheless, transchelation found in an EDTA challenging experiment was lower for TAFC (3−5% TAFC vs 13% *C7* after 7 days) despite its lower coordination number (6 vs 8).

Although further research is warranted, our study shows that the use of macrocyclic structure leads to considerably improved

DOI: 10.1021/acs.molpharmaceut.5b00128
Mol. Pharmaceutics 2015, 12, 2142−2150

in vitro stability compared to DFO. A limitation of the study is that DFO cannot be used to generate a trimeric structure. Thus, *in vivo* comparison of both chelating systems is difficult because not only the chelator system would change but also the number of targeting moieties. Based on these changes the *in vivo* properties are not only correlated to the different chelators but also are influenced by the different structures. Therefore, it was decided for this proof of principle study to restrict comparison to *in vitro* assays where it is assumed that these differences have only minor effects. Anyway, to our knowledge this is the first report where a ^{89}Zr-labeled macrocyclic bifunctional chelating system conjugated to a target vector is studied *in vivo* including biodistribution and PET imaging. Both, the *in vitro* and *in vivo* studies of [^{89}Zr]TAFC and [^{89}Zr]FSC(succ-RGD)$_3$ demonstrated very promising results. However, small peptides, even though an excellent model for this evaluation based on their rapid pharmacokinetics, are certainly not the most suitable application for this concept. Nevertheless, for larger targeting vectors (such as antibodies or antibody fragments), due to their slower pharmacokinetics, FSC system could be a very interesting alternative for ^{89}Zr-labeling to currently used bifunctional chelators. At the moment, mono- and diacetylated FSC are under investigation, which may, due to the reduced free valences, better suit the application with higher molecular weight targeting vector systems.

CONCLUSION

Versatile conjugation strategies of FSC were explored using RGD as model peptide and quantitative labeling with ^{89}Zr was achieved successfully. Excellent *in vitro* and *in vivo* stability of [^{89}Zr]TAFC and [^{89}Zr]FSC-RGD conjugates were demonstrated. These results led us to conclude that FSC is a novel promising chelator for the development of ^{89}Zr-based PET imaging agents.

ASSOCIATED CONTENT

Supporting Information

Figure S1 showing the representative chromatograms of ITLC of ^{89}Zr-oxalate and [^{89}Zr]TAFC. The Supporting Information is available free of charge on the ACS Publications website at DOI: 10.1021/acs.molpharmaceut.5b00128.

AUTHOR INFORMATION

Corresponding Author

*Address: Anichstr. 35, A-6020 Innsbruck, Austria. Phone: +43 (0)512 504 80951. Fax: +43 (0)512 504 6780951. E-mail: clemens.decristoforo@uki.at.

Notes

The authors declare no competing financial interest.

ACKNOWLEDGMENTS

We acknowledge the financial support of the Austrian Science Foundation (FWF) grant P 25899-B23 and the China Scholarship Council.

REFERENCES

(1) Fischer, G.; Seibold, U.; Schirrmacher, R.; Wangler, B.; Wangler, C. ^{89}Zr, a radiometal nuclide with high potential for molecular imaging with PET: chemistry, applications and remaining challenges. *Molecules* **2013**, *18*, 6469−6490.

(2) Deri, M. A.; Zeglis, B. M.; Francesconi, L. C.; Lewis, J. S. PET imaging with ^{89}Zr: From radiochemistry to the clinic. *Nucl. Med. Biol.* **2013**, *40*, 3−14.

(3) Chang, A. J.; DeSilva, R.; Jain, S.; Lears, K.; Rogers, B.; Lapi, S. ^{89}Zr-radiolabeled trastuzumab imaging in orthotopic and metastatic breast tumors. *Pharmaceuticals* **2012**, *5*, 79−93.

(4) Aerts, H. J.; Dubois, L.; Perk, L.; Vermaelen, P.; van Dongen, G. A.; Wouters, B. G.; et al. Disparity between in vivo EGFR expression and ^{89}Zr-labeled cetuximab uptake assessed with PET. *J. Nucl. Med.* **2009**, *50*, 123−131.

(5) Holland, J. P.; Divilov, V.; Bander, N. H.; Smith-Jones, P. M.; Larson, S. M.; Lewis, J. S. ^{89}Zr-DFO-J591 for immunoPET of prostate-specific membrane antigen expression in vivo. *J. Nucl. Med.* **2010**, *51*, 1293−1300.

(6) Zeglis, B. M.; Mohindra, P.; Weissmann, G. I.; Divilov, V.; Hilderbrand, S. A.; Weissleder, R.; et al. Modular strategy for the construction of radiometalated antibodies for positron emission tomography based on inverse electron demand diels−alder click chemistry. *Bioconjugate Chem.* **2011**, *22*, 2048−2059.

(7) van Rij, C. M.; Sharkey, R. M.; Goldenberg, D. M.; Frielink, C.; Molkenboer, J. D.; Franssen, G. M.; et al. Imaging of prostate cancer with immuno-PET and immuno-SPECT using a radiolabeled anti-EGP-1 monoclonal antibody. *J. Nucl. Med.* **2011**, *52*, 1601−1607.

(8) Heskamp, S.; van Laarhoven, H. W.; Molkenboer-Kuenen, J. D.; Franssen, G. M.; Versleijen-Jonkers, Y. M.; Oyen, W. J.; et al. ImmunoSPECT and immunoPET of IGF-1R expression with the radiolabeled antibody R1507 in a triple-negative breast cancer model. *J. Nucl. Med.* **2010**, *51*, 1565−1572.

(9) Perk, L. R.; Vosjan, M. J.; Visser, G. W.; Budde, M.; Jurek, P.; Kiefer, G. E.; et al. p-Isothiocyanatobenzyl-desferrioxamine: a new bifunctional chelate for facile radiolabeling of monoclonal antibodies with zirconium-89 for immuno-PET imaging. *Eur. J. Nucl. Med. Mol. Imaging* **2010**, *37*, 250−259.

(10) Tinianow, J. N.; Gill, H. S.; Ogasawara, A.; Flores, J. E.; Vanderbilt, A. N.; Luis, E.; et al. Site-specifically ^{89}Zr-labeled monoclonal antibodies for ImmunoPET. *Nucl. Med. Biol.* **2010**, *37*, 289−97.

(11) Patra, M.; Bauman, A.; Mari, C.; Fischer, C. A.; Blacque, O.; Häussinger, D.; et al. An octadentate bifunctional chelating agent for the development of stable zirconium-89 based molecular imaging probes. *Chem. Commun.* **2014**, *50*, 11523−11525.

(12) Deri, M. A.; Ponnala, S.; Zeglis, B. M.; Pohl, G.; Dannenberg, J. J.; Lewis, J. S.; et al. An alternative chelator for ^{89}Zr radiopharmaceuticals: radiolabeling and evaluation of 3, 4, 3-(LI-1, 2-HOPO). *J. Med. Chem.* **2014**, *57*, 4849−4860.

(13) Guérard, F.; Lee, Y. S.; Brechbiel, M. W. Rational design, synthesis, and evaluation of tetrahydroxamic acid chelators for stable complexation of zirconium (IV). *Chemistry* **2014**, *20*, 5584−5591.

(14) Pandya, D. N.; Pailloux, S.; Tatum, D.; Magda, D.; Wadas, T. J. Di-macrocyclic terephthalamide ligands as chelators for the PET radionuclide zirconium-89. *Chem. Commun.* **2015**, *51*, 2301−2303.

(15) Ma, M. T.; Meszaros, L. K.; Paterson, B. M.; Berry, D. J.; Cooper, M. S.; Ma, Y. Tripodal tris (hydroxypyridinone) ligands for immunoconjugate PET imaging with ^{89}Zr^{4+}: comparison with desferrioxamine-B. *Dalton Trans.* **2015**, *44*, 4884−4900.

(16) Liu, S.; Edwards, D. S. Bifunctional chelators for therapeutic lanthanide radiopharmaceuticals. *Bioconjugate Chem.* **2001**, *12*, 7−34.

(17) Knetsch, P. A.; Zhai, C.; Rangger, C.; Blatzer, M.; Haas, H.; Kaeopookum, P.; et al. [^{68}Ga]FSC-(RGD)$_3$, a trimeric RGD peptide for imaging $\alpha_v\beta_3$ integrin expression based on a novel siderophore derived chelating scaffold− synthesis and evaluation. *Nucl. Med. Biol.* **2015**, *42*, 115−122.

(18) Zhai, C.; Summer, D.; Rangger, C.; Haas, H.; Decristoforo, C.; Fusarinine, C. a fast, high specific activity, wide pH range, and stable multivalent bifunctional siderophore chelator for radiolabeling with gallium-68. *J. Labelled Comp. Radiopharm.* **2015**, *58*, 209−214.

(19) Petrik M., Zhai C., Novy Z., Urbanek L., Haas H., Decristoforo C. In vitro and in vivo comparison of selected ^{68}Ga and ^{89}Zr labelled siderophores. *Nucl. Med. Biol.* Under review.

(20) Petrik, M.; Haas, H.; Schrettl, M.; Helbok, A.; Blatzer, M.; Decristoforo, C. In vitro and in vivo evaluation of selected ^{68}Ga-

DOI: 10.1021/acs.molpharmaceut.5b00128
Mol. Pharmaceutics 2015, 12, 2142−2150

siderophores for infection imaging. *Nucl. Med. Biol.* **2012**, *39*, 361−369.
(21) Knetsch, P. A.; Petrik, M.; Griessinger, C. M.; Rangger, C.; Fani, M.; Kesenheimer, C.; et al. [^{68}Ga]NODAGA-RGD for imaging $\alpha_v\beta_3$ integrin expression. *Eur. J. Nucl. Med. Mol. Imaging* **2011**, *38*, 1303−1312.
(22) Vosjan, M. J.; Perk, L. R.; Visser, G. W.; Budde, M.; Jurek, P.; Kiefer, G. E.; et al. Conjugation and radiolabeling of monoclonal antibodies with zirconium-89 for PET imaging using the bifunctional chelate p-isothiocyanatobenzyl-desferrioxamine. *Nat. Protoc.* **2010**, *5*, 739−743.
(23) Petrik, M.; Haas, H.; Dobrozemsky, G.; Lass-Flörl, C.; Helbok, A.; Blatzer, M.; et al. ^{68}Ga-siderophores for PET imaging of invasive pulmonary aspergillosis: proof of principle. *J. Nucl. Med.* **2010**, *51*, 639−645.
(24) Haubner, R.; Gratias, R.; Diefenbach, B.; Goodman, S. L.; Jonczyk, A.; Kessler, H. Structural and functional aspects of RGD-containing cyclic pentapeptides as highly potent and selective integrin $\alpha_v\beta_3$ antagonists. *J. Am. Chem. Soc.* **1996**, *118*, 7461−7472.
(25) Haubner, R.; Maschauer, S.; Prante, O. PET radiopharmaceuticals for imaging integrin expression: tracers in clinical studies and recent developments. *Biomed. Res. Int.* **2014**, 871609.
(26) Haubner, R.; Decristoforo, C.; Radiolabelled, R. G. D. peptides and peptidomimetics for tumour targeting. *Front. Biosci.* **2009**, *14*, 872−86.
(27) Gaertner, F. C.; Kessler, H.; Wester, H. J.; Schwaiger, M.; Beer, A. J. Radiolabelled RGD peptides for imaging and therapy. *Eur. J. Nucl. Med.* **2012**, *39* (Suppl 1), S126−S138.
(28) Liu, S. Radiolabeled multimeric cyclic RGD peptides as integrin $\alpha_v\beta_3$ targeted radiotracers for tumor imaging. *Mol. Pharmaceutics* **2006**, *3*, 472−487.
(29) Dumont, R. A.; Deininger, F.; Haubner, R.; Maecke, H. R.; Weber, W. A.; Fani, M. Novel ^{64}Cu-and ^{68}Ga-labeled RGD conjugates show improved PET imaging of $\alpha_v\beta_3$ integrin expression and facile radiosynthesis. *J. Nucl. Med.* **2011**, *52*, 1276−1284.
(30) Chen, X.; Park, R.; Tohme, M.; Shahinian, A. H.; Bading, J. R.; Conti, P. S. MicroPET and autoradiographic imaging of breast cancer α_v-integrin expression using ^{18}F-and ^{64}Cu-labeled RGD peptide. *Bioconjugate Chem.* **2004**, *15*, 41−49.
(31) Guérard, F.; Lee, Y.-S.; Tripier, R.; Szajek, L. P.; Deschamps, J. R.; Brechbiel, M. W. Investigation of Zr (IV) and ^{89}Zr (IV) complexation with hydroxamates: progress towards designing a better chelator than desferrioxamine B for immuno-PET imaging. *Chem. Commun.* **2013**, *49*, 1002−1004.

DOI: 10.1021/acs.molpharmaceut.5b00128
Mol. Pharmaceutics 2015, 12, 2142−2150